

ANALYSIS OF THREE-LAYER GASKET PERFORMANCE AFFECTED BY FLANGE SURFACE

I Made Gatot Karohika✉

Department of Mechanical Engineering

Udayana University

Bukit Jimbaran str., Badung, Bali, Indonesia, 80361

Department of Mechanical Engineering Master Program

Udayana University

P.B Sudirman str., Denpasar, Bali, Indonesia, 80234

gatot.karohika@unud.ac.id

Shigeyuki Haruyama

Management of Technology Department

Yamaguchi University

2-16-1 Tokiwadai, Ube-shi, Yamaguchi, Japan, 755-8611

✉Corresponding author

Abstract

Gaskets are components that play a very important role in piping connections to prevent leakage. Several factors affect the performance of the gasket, one of which is the contact surface of the flange. The quality of the contact surfaces in the connection also influences the leakage rate of each connection, therefore the gasket sealing performance is assessed by the rate of leakage that occurs. As a result, the surface roughness of the flange has an effect on sealing. This study examines the capability of a three-layer corrugated metal gasket to prevent leakage when the outside layer thickness and flange roughness are adjusted. The feature of three-layer corrugated metal gasket was elucidated using the finite element analysis (FEA) and experimental method. The leak rate was tested using a helium leak quantity test experimentally. The gasket was constructed with oxygen-free copper (C1020) as the outside layer and SUS304 as the base layer, and it was structured in a three-layer pattern with no bonding. A mold press was used to make the gasket. The simulation method applies finite element analysis software to investigate the correlation between contact stress, contact width, surface thickness and surface roughness. The projected results matched the experiment results fairly well. A three-layer corrugated metal gasket shows improvement capability to prevent leakage than a single gasket (standard). The gasket three-layer shows sealing performance improvement that leakage did not occur in low axial force 40 kN for all surface roughness test. In terms of sealing, a three-layer gasket with a low thickness ratio works well. Surface roughness of the flange has no influence on the three-layer gasket.

Keywords: leakage, performance, surface, roughness, contact width, contact stress, thickness, sealing, gasket, corrugated.

DOI: 10.21303/2461-4262.2022.002290

1. Introduction

A bolted flange connection is a complicated mechanical system with components that must be carefully chosen and constructed to enable dependable sealing under a variety of operating circumstances. The proper operation of the joint depends on all of the numerous components of the completed bolted flange connection [1–5].

The pipework, or vessels, the flanges, gaskets, and bolts are the components. The design and assembly of the joint, in addition to the components themselves, are crucial to the joint's long-term performance. The combination of the use of FEM and experimental testing has been widely used to determine the effect of several factors on the performance of gaskets, such as the use of PTFE gasket material which is influenced by external bending moment and internal pressure [6], acoustic method to measure leakage [7]. Measurement of contact stress by comparing the results of FEM with pressure sensitive paper [8, 9], the use of various types of gas to measure leakage in the packing ring [10], the effect of compressive stress, medium pressure and surface topography (gasket surface roughness) on the leakage rate [11]. The effect of flat gasket thickness on deformation [12] and the use of ANSYS software to test the effectiveness of the PPNC method as a measure of flat gasket performance [13]. A gasket is used to produce and maintenance a static seal between two flanges that link a series of mechanical components and hold a range of fluids (liquids and/or gases) [14].

The simulation approach has long been used as a dependable tool for conducting many types of digital tests. Before any manufacturing movements are made, the performance and cost of additives can be regulated. The benefit of numerical simulation is that structural changes that must adhere to a preferred specification or output can be performed immediately, and the simulation can be rerun multiple times until the desired result is achieved. In addition to numerical evaluations, experimental work is required to validate affirmative requirements. Because numerical observation is an assumed approach, a great deal of research has gone into determining the source of this disparity, which is a serious flaw in numerical simulation not only in the seal, gasket simulations [15, 16], but also in other simulation domains.

The condition of the contact surface between the flange and the gasket influences the sealing performance of the gasket, which decreases as the smoothness of the contact surface decreases [17, 18]. Efforts to improve gasket performance are carried out either by coating [19–21], laminating [22], or redesigning [23]. Based on this, in this study, let's try to improve the performance of the gasket from previous studies [17] by layering the outside with cooper which is also influenced by the surface roughness of the flange so that the performance of the three-layer gasket is indeed better than the previous gasket.

2. Materials and methods

2. 1. Gasket simulation

The contact mechanism between the 25A-size metal gasket and the rough flange was described by a simulation study. The link between the surface roughness and surface thickness parameter to the contact stress, as well as the contact width, was determined using this method. A mold press was used to create the gasket for this experiment. The gasket section consists of a curved shape and a flat shape. The flat sides of the gasket produced an elastic action when it was tightened to the flange. On both sides of the flange, it was believed to be rough. The gasket was pushed in an axial direction by the flange. SUS304 was chosen as the base layer gasket. The outside layer was made of C1020, and the flange was made of SS400. **Table 1** shows the material qualities in detail.

Table 1

Material engineering data used in simulation analysis

Materials	Nominal Stress (σ), MPa	Tangent Modulus, MPa	Modulus of Elasticity (E), GPa	Poisson ratio (ν)
SUS304	398.83	1900.53	210	0.3
SS400	240	1000	206	0.3
C1020	195	1360	136	0.31

In this study, the flange with 2 surface roughness values: 2.5 μm and 3.5 μm . The flange roughness was modeled base on average roughness (Ra) measurement data from a Handysurf E-35B.

Using FEM, MSC Marc. Software, the elastoplastic behavior of the gasket is computed. The loading condition is shown in **Fig. 1**. The upper and lower dies and flange displacement is in the axial direction on the gasket with a continuous increasing step of displacement U_X is implemented. The calculation using 2 dimensional analysis, axisymmetric solid components, isoperimetric quadrilateral type 10.

In this study, the material model use linear hardening law (**Fig. 2**). The contact width calculated by multiplying the amount of nodes with contact stress in plastic condition by the element size (**Fig. 3**). If the node contact stress is 0 MPa, indicates there is no contact. If the node contact stress between of 0-195 MPa indicates elastic contact. The value of contact stress of 195 MPa and bigger indicates plastic contact.

To begin, Solidworks software was used to create 2 dimensional parametric models of the flange and gasket. Hypermesh is applied to create automatic meshing on gaskets and flange models imported from Solidworks. Because the gasket and flange part has a rectangular portion, let's select a quadrilateral mesh. The procedure file was set up to pre-process the data and run the model on MSC MARC software. Following the completion of the FEM analysis, a TXT file with the

analysis findings can be generated. At each peak point, the result provides the contact status, contact width, contact stress and force. A multi-step MACRO command is used to calculate the contact width vs the loading force at each peak positions.

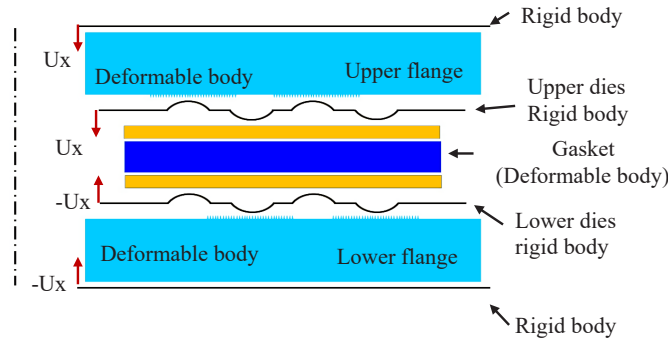


Fig. 1. Analysis model

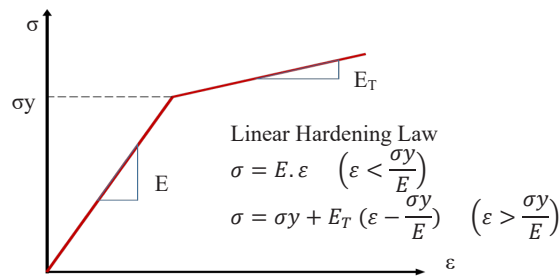


Fig. 2. Material model

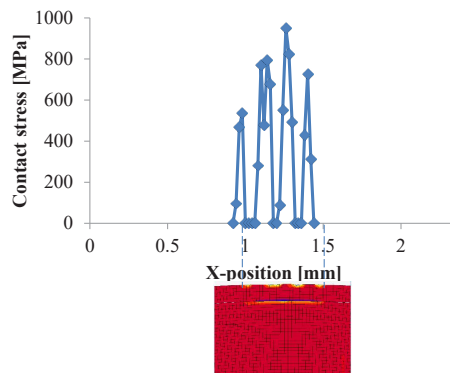


Fig. 3. Horizontal contact stress

Fig. 4 depicts a three sheet metal structure with T_s standing for outside layer thickness, T_b for base metal thickness, and T_g for total thickness gasket. The settings for gasket material, flange, and curve are shown in Fig. 5. The gasket pattern created by the press mold machine was pushed along the axial direction. The loading process by tighten the flange to gasket, as shown in Fig. 6. The contact between the base metal (SUS304) and the outside layer (C1020) is unfixable (unbonding). On both sides, the gasket and the flange were believed to be deformable. A 400-MPa mode design [17] was employed in this simulation. Thickness ratios of 0.1/1.5, 0.2/1.5, 0.4/1.5, and 0.5/1.5 were studied, as well as two flange surface roughness levels of 2.5 μm and 3.5 μm .

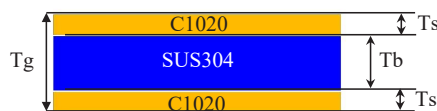


Fig. 4. Sheet metal with three layers

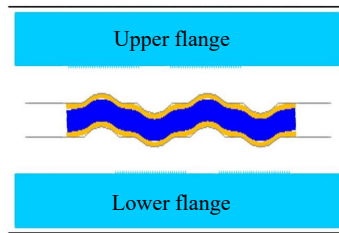


Fig. 5. Simulation of forming

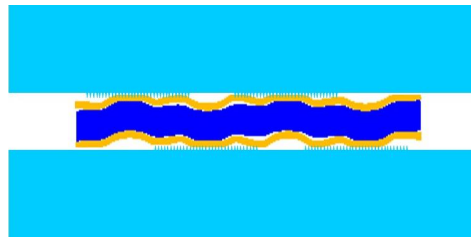


Fig. 6. Simulation of tightening

2. 2. Manufacturing of Gaskets

A mold press was used to make the gasket. The shape of the gasket is achieved by forcing the raw material into a die with a punch. The gasket was made with C1020 as the outside layer and SUS304 as the inside layer, and it was assembled in a three-layer structure without the use of any adhesives. Die dimensions based on optimum single SUS304 400-MPa modes. As illustrated in Fig. 7, the dies are used to create the material gasket. The forming process was carried out using a UH-1000 KNI universal testing machine. Fig. 8 depicts the gasket before the forming process and the gasket after the forming process.



Fig. 7. The upper and lower dies

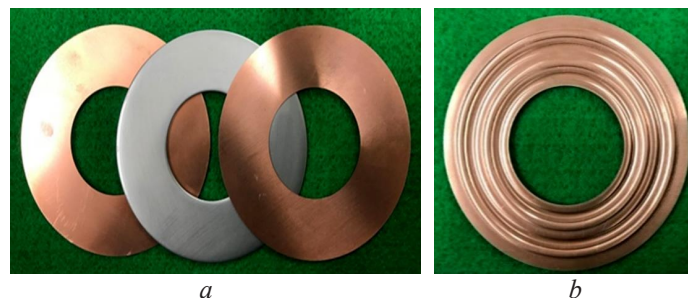


Fig. 8. Three-layer metal gasket: *a* – before forming; *b* – after forming

2. 3. Measurement of Flange Surface Roughness

The sealing performance is influenced by the surface roughness. The flange surface roughness used the JISB0601-2001 standard. The surface roughness measurement experimental setup is shown in Fig. 9. The surface roughness was measured with a Handysurf E-35B. The all data that consist of profile curve, parameter values, and measurement conditions can be sent straight to a computer with this configuration.

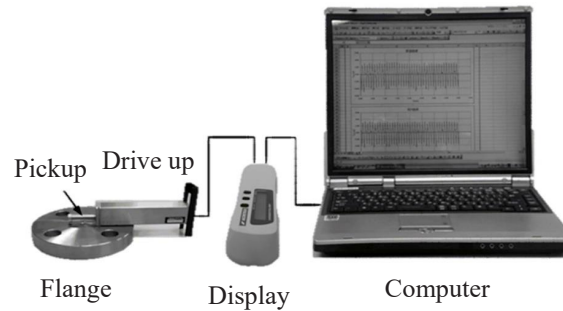


Fig. 9. Measurement setup for surface roughness

The processing of the data of the output result (R_a , R_z and other parameters) was done in Microsoft Excel. Additionally, the output result can be received as a roughness curve.

The result of a surface roughness measurement is shown in **Fig. 10**.

With the help of the SolidWork program, the flange roughness (R_a) values: $2.5 \mu\text{m}$ and $3.5 \mu\text{m}$, was drawn.

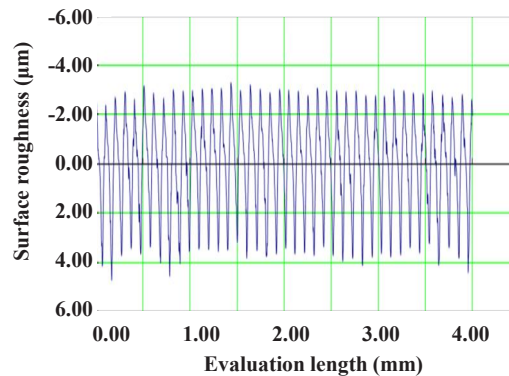


Fig. 10. Roughness curve

2. 4. Measurement of Leak Quantity

In this test was employed a general-purpose flange based on JIS B2220 as shown in **Fig. 11**.



Fig. 11. General-purpose 25A flange

The helium leak rate quantity was evaluated to determine correlation of the axial force and leakage quantity is shown schematically in **Fig. 12**.

The quantitative measurements of helium leakage were taken according to the JIS Z2330 and JIS Z2331 standards, as was describe in the previous research [23].

The relationship between loading force and helium leak rate is used to evaluate gasket performance. The flange was clamped with four bolts, loading forces were measured at 40, 60, 80, 100, and 120 KN.

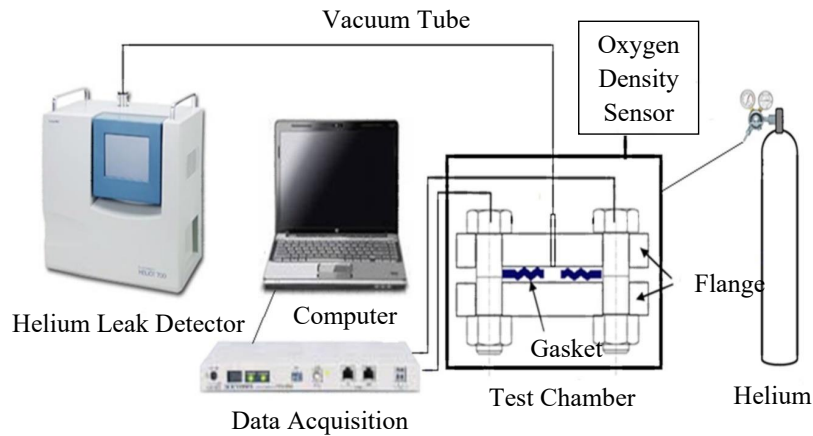


Fig. 12. A helium leak detection system design

3. Result and discussions

The relation between contact width, contact stress, axial force of a three-layer metal gasket for convex 1, 2, 3, and 4 in any axial/loading force are shown in Fig. 13. Fig. 13 demonstrates that convex 2 and 3 had higher average contact stress and contact width than convex 1 and 4. As a result, the investigation concentrated on middle convex (2 and 3), namely as the bottom and upper contacts, respectively.

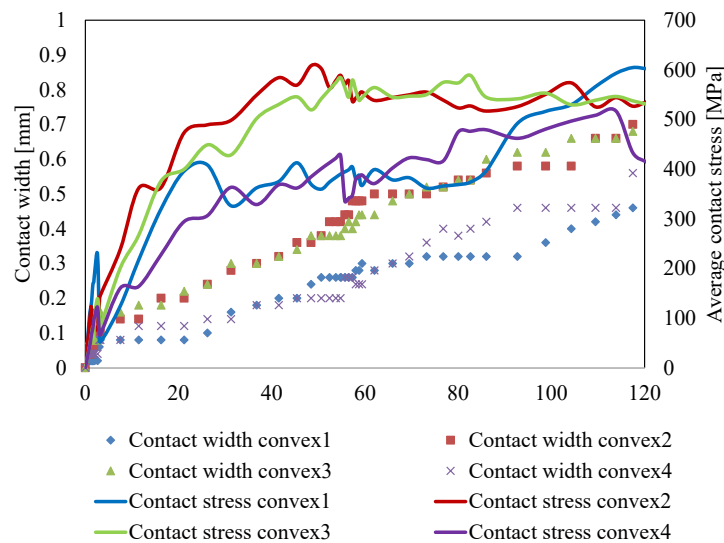


Fig. 13. The relation contact width, contact stress, axial force

The simulation result for contact width of a gasket, flange surface roughness $3.5 \mu\text{m}$ is shown in Fig. 14. The contact width rises as the axial force increases, as shown in this diagram. The maximum and lowest slopes were found in a gasket with a thickness ratio of 0.1/1.5 and 0.4/1.5, respectively.

For average contact stress, Fig. 15 illustrates the simulation result for the upper and lower contact of a gasket in contact with flanges with surface roughness values of $3.5 \mu\text{m}$. For various thickness ratios, the contact stress for a gasket was similar for both the top and bottom contacts. However, a gasket with a thickness ratio of 0.1/1.5 had the highest tendency of all the gaskets tested. The average contact stress increases dramatically as the axial force increases, as shown in the graph.

The simulation result for contacts width of a gasket for flanges with a surface roughness of $2.5 \mu\text{m}$ is shown in Fig. 16. The contact width rises as the axial force increases, as shown in this diagram. The maximum and lowest slopes were found in a gasket with a thickness ratio of 0.1/1.5 and 0.4/1.5, respectively.

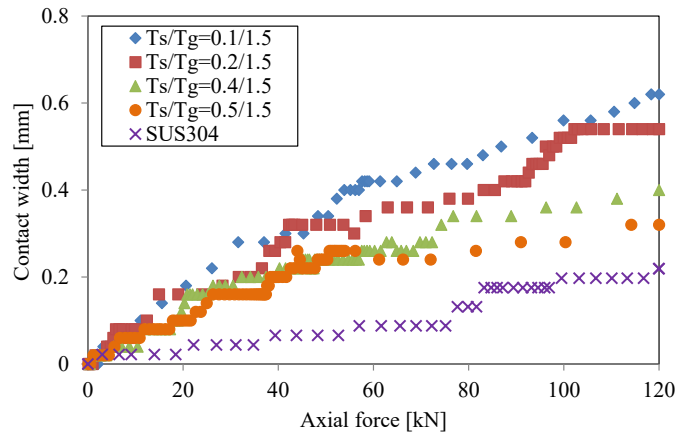


Fig. 14. Contact width for a gasket in 400-MPa mode [3.5 μm]

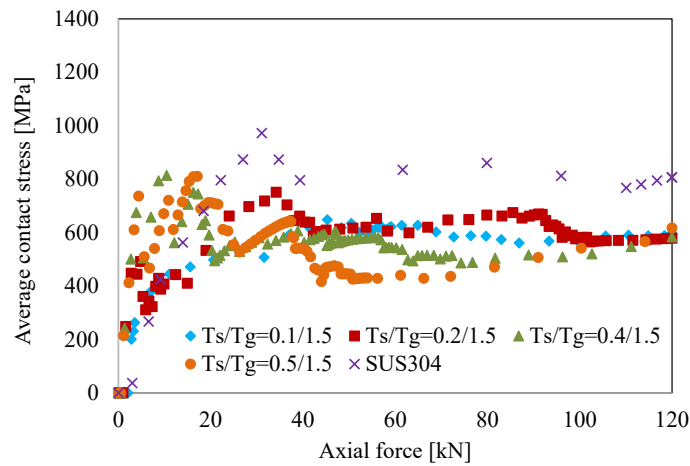


Fig. 15. Gasket contact stress in 400-MPa mode [3.5 μm]

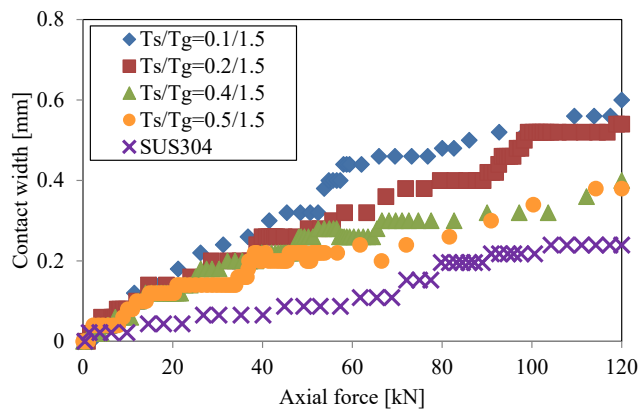


Fig. 16. Gasket contact width [2.5 μm]

The average contact stress of a gasket in contact with flanges roughness 2.5 m is shown in Fig. 17. For various thickness ratios, the contact stress for a gasket was similar for both the top and bottom contacts. However, a gasket with a thickness ratio of 0.1/1.5 had the highest tendency of all the gaskets tested. The average contact stress increases dramatically as the axial force increases, as shown in the graph.

The contact width widened as the axial force increased, as seen in the diagram. It can be seen that the contact width expanded dramatically when the axial force rose from 0 to 50 kN. Surface convex contact stress is a significant plastic contact stress condition in this range. The contact

stress of the flat area is elastic condition, and the phenomenon fulfills the elastic stress requirement, causing the metal gasket undergo spring back. However, as the axial force increases from 50 to 120 kN, the contact width widens. The elastic and plastic regions are mixed due to the stress distribution of the flat area between convex. The spring-back effect is reduced by the plastic contact stress distribution in the region between convex contacts. As a result, the value of contact stress is reduced, and the graph of contact stress tends to move down. The plastic area increases as the axial force increases, while the contact stress tends to remain constant.

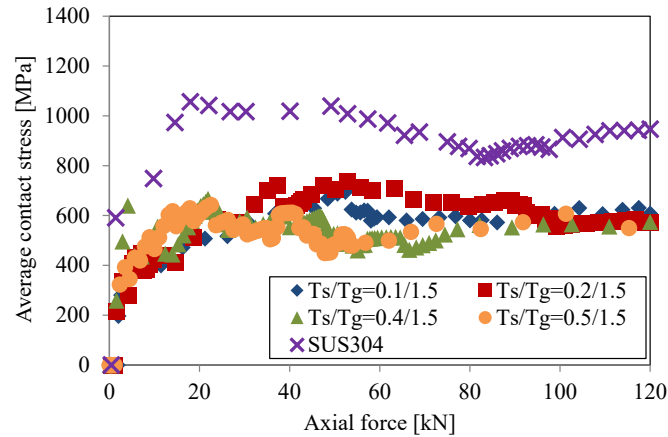


Fig. 17. Gasket average contact stress [2.5 μm]

The helium leak quantity test for a gasket when contacted a flange with surface roughness Ra 3.5 μm is shown in Fig. 18. At 40 axial force, none of the three-layer gaskets leaked. At 100 axial force, the gasket made of a single material SUS304 does not leak. Three-layer gaskets perform better than SUS304 gaskets in terms of sealing.

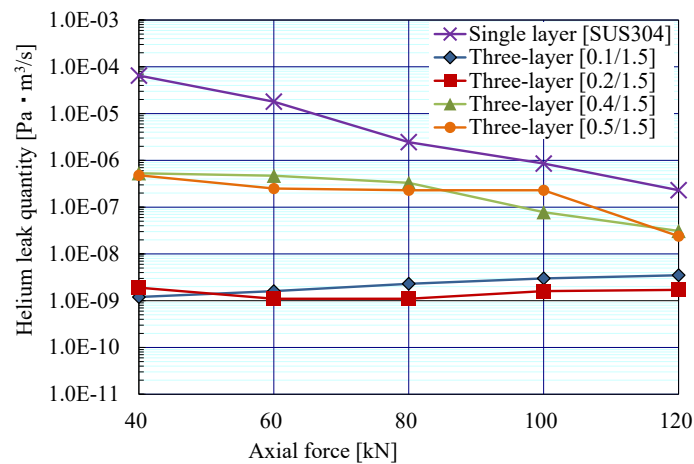


Fig. 18. Helium leak quantity test result (Ra 3.5 μm)

The helium leak quantity test for a gasket when contacted a flange with surface roughness Ra 2.5 μm is shown in Fig. 19. At 40 axial force, none of the three-layer gaskets leaked, but gasket single material still leaked. At 80 axial force, the gasket made of single material SUS304 does not leak. The three-layer gasket seals better than the SUS304 gasket.

The modeling results and experimental data were found to be in good agreement. Theoretically, as contact width and contact tension increase, helium leakage decreases. A previous study [17] found that when the contact width is 0.195 mm, there is no leakage on 80 kN. The three-layer metal gasket $T_s/T_g = 0.5/1.5$ found in this investigation already started not leak in force 40kN and contact width 0.2 mm. In other words, it is possible to conclude that the three-layer of the

gasket performs preferable than the single SUS304 gasket. In addition, the findings of the helium leakage tests demonstrate that the $T_s/T_g = 0.1/1.5$ three-layer gasket model outperforms the others.

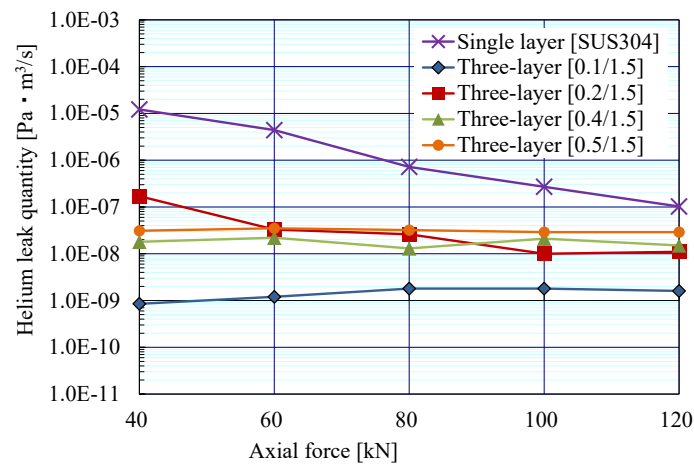


Fig. 19. Helium leak quantity (Ra 2.5 μm)

Because the simulation and experimental results are similar, it is possible to say that our simulation model is close to the real model.

This research was tested in conditions of room temperature and fluid gas without the effect of additional pressure, and because the research is carried out in a laboratory, the influence of outside interference can be minimized. In application on real conditions such as hot water pipe connections, the effect of temperature and inner pressure increased due to hot fluid flowing in the pipe needs to be further research.

4. Conclusions

The novelty of the gasket is in its new design feature, the use of three layers with varying thickness of the gasket layer. Simulation test results which are also reinforced by experimental results show that the performance of the three-layer gasket is better than the single gasket SUS304, in detail it can be described as follows:

1. The gasket three-layer shows improvement capability to prevent leakage than a single gasket based on the helium leakage test.
2. The gasket three-layer showed improved sealing performance so that no leakage occurred at low axial forces at 40 kN to 120 kN for all surface roughness tests.
3. In general, an increase in surface roughness causes a decrease in the contact width of the gasket as well as the contact stress. In three layers gasket, a lower thickness ratio (thinner surface) provides a greater contact width and contact stress, so the $T_s/T_g = 0.1/1.5$ three layers gasket model is recommended as it outperforms the others.

References

- [1] Li, X., Yao, C., Li, J. (2016). Research on Tightness Performance of Corrugated Gasket Bolted Flanged Connections System. Volume 1B: Codes and Standards. doi: <https://doi.org/10.1115/pvp2016-63794>
- [2] Wei, Z., Wang, L., Guan, Y., Yao, S., Li, S. (2016). Static metal sealing mechanism of a subsea pipeline mechanical connector. Advances in Mechanical Engineering, 8 (7), 168781401665482. doi: <https://doi.org/10.1177/1687814016654821>
- [3] Hosoya, N., Hosokawa, T., Kajiwara, I., Hashimura, S., Huda, F. (2018). Evaluation of the Clamping Force of Bolted Joints Using Local Mode Characteristics of a Bolt Head. Journal of Nondestructive Evaluation, 37 (4). doi: <https://doi.org/10.1007/s10921-018-0528-7>
- [4] Li, Y., Wang, H. (2020). Study on strength and sealing of a bolted flange joint under complex working conditions. IOP Conference Series: Materials Science and Engineering, 768 (4), 042030. doi: <https://doi.org/10.1088/1757-899x/768/4/042030>
- [5] Jaszak, P. (2021). Prediction of the durability of a gasket operating in a bolted-flange-joint subjected to cyclic bending. Engineering Failure Analysis, 120, 105027. doi: <https://doi.org/10.1016/j.engfailanal.2020.105027>

- [6] Sato, K., Sawa, T., Morimoto, R., Kobayashi, T. (2017). FEM Stress Analysis and Mechanical Characteristics of Bolted Pipe Flange Connections With PTFE Blended Gaskets Subjected to External Bending Moments and Internal Pressure. Volume 2: Computer Technology and Bolted Joints. doi: <https://doi.org/10.1115/pvp2017-65332>
- [7] Sakamoto, S., Azami, T., Nitta, I., Tsukiyama, Y. (2016). Fundamental study of acoustic leakage through a gap between gasket and flange surface. Journal of Advanced Mechanical Design, Systems, and Manufacturing, 10 (4), JAMDSM0067–JAMDSM0067. doi: <https://doi.org/10.1299/jamdsm.2016jamdsm0067>
- [8] Zhang, M., Suo, S., Jiang, Y., Meng, G. (2018). Experimental Measurement Method for Contact Stress of Elastic Metal Sealing Ring Based on Pressure Sensitive Paper. Metals, 8 (11), 942. doi: <https://doi.org/10.3390/met8110942>
- [9] Du, P., Lu, J., Tuo, J., Wang, X. (2019). Research on the Optimization Design of Metallic Gasket Based on DOE Methodology. IOP Conference Series: Materials Science and Engineering, 569 (3), 032027. doi: <https://doi.org/10.1088/1757-899x/569/3/032027>
- [10] Kazeminia, M., Bouzid, A.-H. (2018). Leak prediction through porous compressed packing rings: A comparison study. International Journal of Pressure Vessels and Piping, 166, 1–8. doi: <https://doi.org/10.1016/j.ijpvp.2018.07.012>
- [11] Feng, X., Gu, B., Zhang, P. (2018). Prediction of Leakage Rates Through Sealing Connections with Metallic Gaskets. IOP Conference Series: Earth and Environmental Science, 199, 032090. doi: <https://doi.org/10.1088/1755-1315/199/3/032090>
- [12] Gawande, S. H. (2018). Study on the effect of gasket thickness for bolted gearbox flange joint. SN Applied Sciences, 1 (1). doi: <https://doi.org/10.1007/s42452-018-0030-y>
- [13] Aljuboury, M., Rizvi, M. J., Grove, S., Cullen, R. (2021). A numerical investigation of the sealing performance and the strength of a raised face metallic bolted flange joint. International Journal of Pressure Vessels and Piping, 189, 104255. doi: <https://doi.org/10.1016/j.ijpvp.2020.104255>
- [14] Tang, H. N., Yao, H., Wang, S. J., Meng, X. S., Qiao, H. T., Qiao, J. H. (2017). Numerical simulation of leakage rates of labyrinth seal in reciprocating compressor. IOP Conference Series: Materials Science and Engineering, 164, 012015. doi: <https://doi.org/10.1088/1757-899x/164/1/012015>
- [15] Karohika, I. M. G., Antara, I. N. G. (2019). Gasket Process Parameter in Metal Forming. IOP Conference Series: Earth and Environmental Science, 248, 012044. doi: <https://doi.org/10.1088/1755-1315/248/1/012044>
- [16] Karohika, I. M. G., Antara, I. N. G., Budiana, I. M. D. (2019). Influence of dies type for gasket forming shape. IOP Conference Series: Materials Science and Engineering, 539 (1), 012019. doi: <https://doi.org/10.1088/1757-899x/539/1/012019>
- [17] Haruyama, S., Nurhadiyanto, D., Choiron, M. A., Kaminishi, K. (2013). Influence of surface roughness on leakage of new metal gasket. International Journal of Pressure Vessels and Piping, 111-112, 146–154. doi: <https://doi.org/10.1016/j.ijpvp.2013.06.004>
- [18] Zhang, Q., Chen, X., Huang, Y., Zhang, X. (2018). An Experimental Study of the Leakage Mechanism in Static Seals. Applied Sciences, 8 (8), 1404. doi: <https://doi.org/10.3390/app8081404>
- [19] Nurhadiyanto, D., Mujiyono, Sutopo, Amri Ristadi, F. (2018). Simulation Analysis of 25A-Size Corrugated Metal Gasket Coated Copper to Increase Its Performance. IOP Conference Series: Materials Science and Engineering, 307, 012005. doi: <https://doi.org/10.1088/1757-899x/307/1/012005>
- [20] Nurhadiyanto, D., Amrullah, A. M., Mujiyono, Kurniawati, J. (2020). An Analysis on copper corrosion SUS304 corrugated metal gasket electroplating. Journal of Physics: Conference Series, 1700 (1), 012008. doi: <https://doi.org/10.1088/1742-6596/1700/1/012008>
- [21] Nurhadiyanto, D., Haruyama, S., Mujiyono, M., Sutopo, S., Yunaidi, Y., Surahmanto, F. et. al. (2021). Improved performance of corrugated metal gaskets in boiler's piping system through multilayered coating. Eastern-European Journal of Enterprise Technologies, 6 (1 (114)), 13–20. doi: <https://doi.org/10.15587/1729-4061.2021.245360>
- [22] W. S., W., Soenoko, R., Choiron, M. A., Sonief, A. A. (2019). Sealing performance analysis of composite gaskets made of silicone rubber filled with ramie natural fibers. Journal of Mechanical Engineering and Sciences, 13 (4), 6178–6194. doi: <https://doi.org/10.15282/jmes.13.4.2019.28.0484>
- [23] Karohika, I. M. G., Haruyama, S., Choiron, M. A., Nurhadiyanto, D., Antara, I. N. G., Budiarsa, I. N., Widhiada, I. W. (2020). An Approach to Optimize the Corrugated Metal Gasket Design Using Taguchi Method. International Journal on Advanced Science, Engineering and Information Technology, 10 (6), 2435. doi: <https://doi.org/10.18517/ijaseit.10.6.12992>

Received date 13.03.2022

Accepted date 03.07.2022

Published date 30.07.2022

© The Author(s) 2022

This is an open access article
under the Creative Commons CC BY license

How to cite: Karohika, I. M. G., Haruyama, S. (2022). Analysis of three-layer gasket performance affected by flange surface. EUREKA: Physics and Engineering, 4, 57–66. <https://doi.org/10.21303/2461-4262.2022.002290>